Ion Channel Mimics

Deutsche Ausgabe: DOI: 10.1002/ange.201601852
Internationale Ausgabe: DOI: 10.1002/anie.201601852

Thermal Responsive Ion Selectivity of Uranyl Peroxide Nanocages: An Inorganic Mimic of K^+ Ion Channels

Yunyi Gao, Jennifer E. S. Szymanowski, Xinyu Sun, Peter C. Burns, and Tianbo Liu**

Abstract: *An actinyl peroxide cage cluster, $Li_{48+m}K_{12}(OH)_m[UO_2(O_2)(OH)]_{60}(H_2O)_n$ ($m \approx 20$ and $n \approx 310$; U_{60}), discriminates precisely between Na^+ and K^+ ions when heated to certain temperatures, a most essential feature for K^+ selective filters. The U_{60} clusters demonstrate several other features in common with K^+ ion channels, including passive transport of K^+ ions, a high flux rate, and the dehydration of U_{60} and K^+ ions. These qualities make U_{60} (a pure inorganic cluster) a promising ion channel mimic in an aqueous environment. Laser light scattering (LLS) and isothermal titration calorimetry (ITC) studies revealed that the tailorable ion selectivity of U_{60} clusters is a result of the thermal responsiveness of the U_{60} hydration shells.*

Ion channels are transmembrane proteins with the ability to discriminate between different ions.[1] Their high fidelity towards specific ions plays an essential role in regulating many kinds of cellular processes.[2] Given the broad applicability of ion channels, considerable efforts have been dedicated to investigating ion transport and ion selectivity phenomena.[3] Inorganic molecular clusters with well-defined porous surfaces are ideal model systems, which could refine our understanding of the transport and encapsulation behavior of ions in sub-nanometer pores.[4] The ion selectivity of inorganic capsules can be influenced by properties of the capsule's interior structure,[5] the flexibility of surface pores, and exterior stimuli arising from the bulk media.[6]

Actinyl peroxide cage clusters, with nanopores of various sizes and rigid structure, are promising candidates for this study. Understanding the properties of uranium-based nanomaterials is also fundamental for developing an advanced nuclear fuel cycle.[7] $Li_{48+m}K_{12}(OH)_m[UO_2(O_2)(OH)]_{60}(H_2O)_n$ ($m \approx 20$ and $n \approx 310$; U_{60}),[8] demonstrates selective permeability for Na^+ and K^+ ions.[9] However, making U_{60} clusters differentiate between Na^+ and K^+ ions, which are almost identical in size, remains a challenge. As the morphology of U_{60} surface pores is fixed, controlling its hydration shells may be the only way to selectively modify the permeability of U_{60} cages with respect to certain ions. While there is substantial evidence for the significance of hydration shells,[10] few experimental models have attempted to modify this characteristic in pursuit of controlled ion selectivity. Tuning the hydration shells of U_{60} can be achieved simply by regulating the temperature of the aqueous medium. Herein, we present the thermally responsive properties of U_{60}, and the corresponding effect on ion selectivity. It has been demonstrated that U_{60} clusters self-assemble into hollow, spherical, single-layered "blackberry" structures in response to counterion-mediated attraction (Figure 1).[9,11] This behavior is shared with other hydrophilic macroions.[12] The size of the blackberry is controlled by the effective charge of macroions,[12c] solvent polarity,[12d] the type of counterions employed, and additional salts.[12e] The preference of U_{60} clusters for a specific type of counterion can be determined by comparing the sizes of assemblies. Since blackberry formation is charge regulated, size of the cluster does not change significantly with temperature.[12] Interestingly, the behavior of U_{60} clusters is not consistent with this observation.

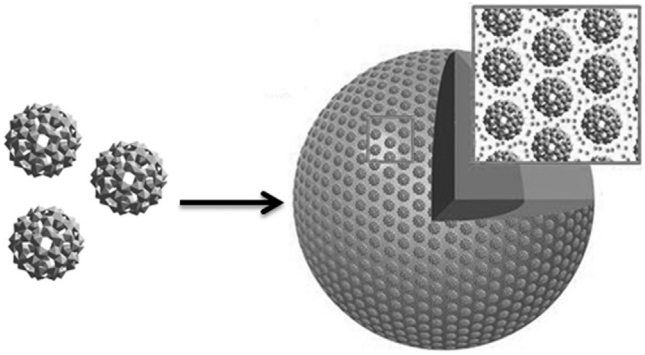

Figure 1. U_{60} clusters and their self-assembled blackberry structures. Inset: dots in the void space between clusters represent counterions.

Small amounts of alkali salt solutions were titrated into U_{60} solutions (1.0 mg mL^{-1}, 3.0 mL) at room temperature (Group 1, same volume and concentration applied to all groups; Figure 2). The concentration of additional alkali salts was 5 mM, with an approximate 1:130 molar ratio of U_{60} with respect to additional couterions. U_{60} precipitated quickly after titration of NaCl into the solution, whereas U_{60} precipitated gradually with CsCl. In the presence of KCl and RbCl, large assemblies were formed with U_{60}. The hydrodynamic radius (R_h) and radius of gyration (R_g) of the assemblies were obtained by dynamic light scattering (DLS) and static light scattering (SLS) measurements after stabilization of the scattering intensity (Figure 2; Supporting Information,

[*] Y. Gao, X. Sun, Prof. Dr. T. Liu
Department of Polymer Science, University of Akron
Akron, OH 44325 (USA)
E-mail: tliu@uakron.edu
J. E. S. Szymanowski, Prof. Dr. P. C. Burns
Department of Civil Engineering and Geological Sciences, University of Notre Dame
Notre Dame, IN 46556 (USA)
E-mail: pburns@nd.edu

Supporting information for this article can be found under: http://dx.doi.org/10.1002/anie.201601852.

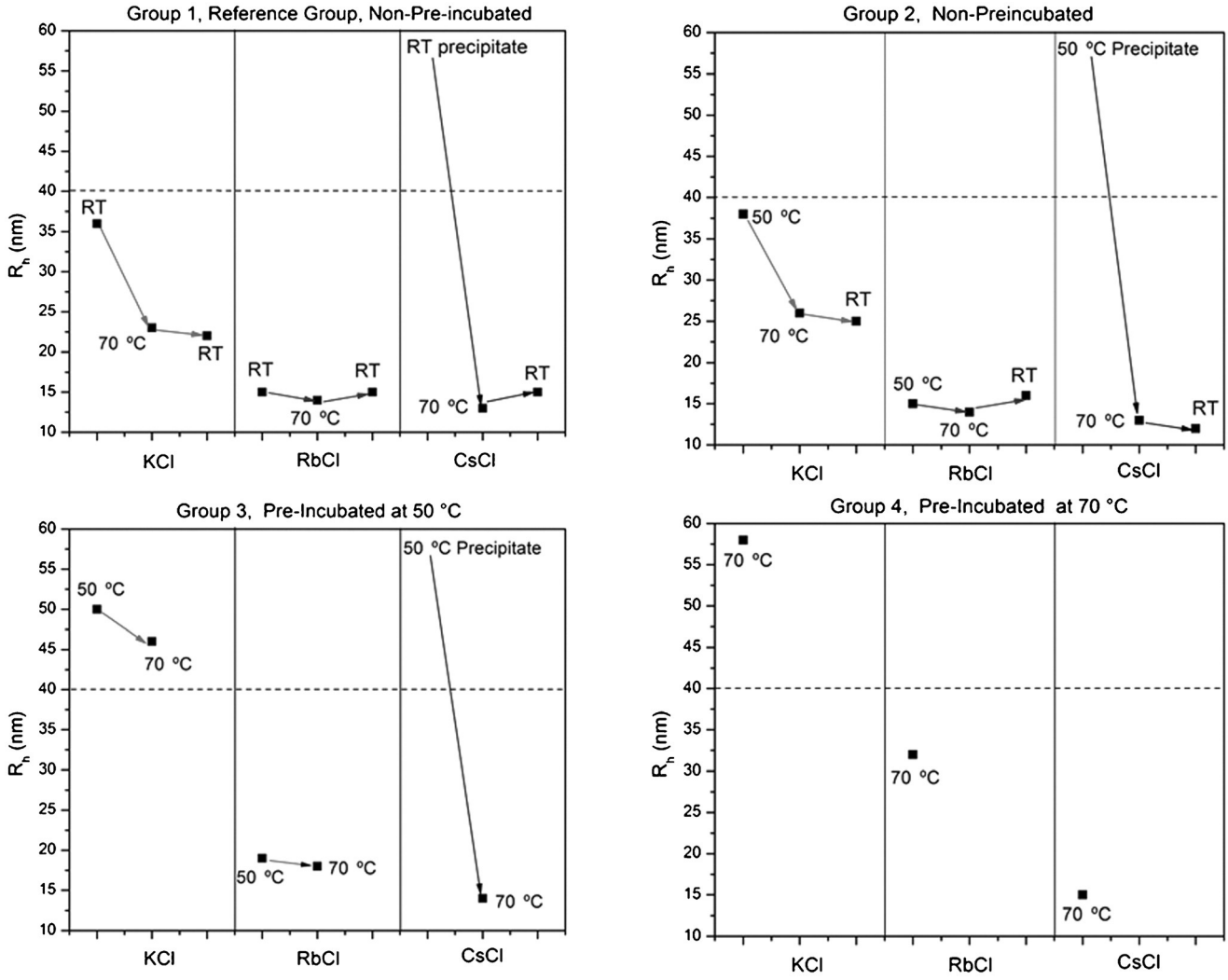

Figure 2. Change of U_{60} assembly sizes (R_h) with additional counterions (molar ratio of U_{60}:K^+/Rb^+/Cs^+, ca. 1:130) upon heating at different temperatures. For Group 1, the solutions were initially titrated and held at room to allow blackberry formation. Subsequently, the solutions were heated to 70°C and then returned to room temperature. For Group 2, the solutions were initially titrated at room temperature and held at 50°C for blackberry formation, followed by the same thermal sequence conducted for Group 1. In Group 3 and 4, the U_{60} solutions were pre-incubated at 50°C/70°C for 3 days before titration.

Tables S1–S4). A ratio of $R_h/R_g \approx 1$ indicates the formation of hollow, spherical "blackberry" structures (for example, $R_h \approx R_g \approx 36$ nm for a U_{60}/KCl solution). As expected the R_h of U_{60}/KCl was larger than that for U_{60}/RbCl because K^+ ions can penetrate the surface pores of U_{60}, thereby lowering the effective charge of U_{60}[9] and allowing formation of larger assemblies.

After blackberry formation at room temperature, the Group 1 solutions were heated to 70°C. After 2 weeks, a number of observations were made. 1) Precipitates in both U_{60}/NaCl and U_{60}/CsCl solutions disappeared and the solutions become clear again, indicating that the U_{60} clusters become more soluble at higher temperatures. The U_{60}/CsCl solution retained strong scattering intensity, indicating the presence of large species. The measured values of $R_h \approx R_g \approx 14$ nm suggest that blackberry structures exist. However, the U_{60}/NaCl solution showed a very low scattered intensity after being incubated at 70°C, indicating no assembly formation. 2) While the radii of U_{60}/RbCl assemblies remained stable at about 15 nm, the assembly radii of U_{60}/KCl exhibited an obvious drop from 36 to 23 nm. More interestingly, when the solutions returned to room temperature, the assembly size in the U_{60}/KCl solution remained stable for at least 2 weeks (Figure 2).

Several conclusions can be drawn from our observations. Firstly, the reasons for precipitation of U_{60}/NaCl and U_{60}/CsCl are different. The low scattered intensity from the U_{60}/NaCl solution after heating suggests that U_{60} clusters exist as soluble discrete macroions. Precipitation at room temperature is a result of the aggregation of single U_{60} clusters. The low solubility of U_{60} clusters here is subject to a reduction in charge when Na^+ ions enter the U_{60} cages.[9] In U_{60}/CsCl solution, U_{60} clusters initially form blackberries, which slowly aggregate and precipitate because of the high ionic strength of

the solution, which makes the blackberries less stable.[13] At 70 °C, these aggregates are redissolved into discrete blackberries, and thus the scattered intensity remains high. Secondly, the size decrease of the KCl blackberries indicates an increase of surface charge density of U_{60}. After incubating the solution at 70 °C, some K^+ ions that have already entered the U_{60} cages migrate out as a result of the higher kinetic energy. Additionally, the hydration shell thickness decreases at higher temperatures;[14] a thinner hydration shell facilitates the escape of K^+. Therefore, the effective charge of U_{60} increases, leading to a stronger repulsion between U_{60} clusters. Consequently, the larger distance between two U_{60} clusters leads to a smaller blackberry size[9] (Figure 3). Furthermore, once K^+ ions are released into the solution, they do not return to the U_{60} cages, which explains why the blackberry size does not change after the solutions return from 70 °C to room temperature. Additional counterions can only interact with discrete U_{60} clusters. Once U_{60} clusters self-assemble into blackberry structures, the overall surface charge on the blackberries screens the entry of free counterions into the U_{60} cages.

To verify the role of the U_{60} hydration shells on the ion transport process, another two sets of U_{60} solutions were prepared. One set was directly titrated with different alkali ions at room temperature (Group 2). The other set was pre-incubated at 50 °C for 3 days before titration (Group 3). Both sets were held at 50 °C after titration. Later the assembly sizes were measured. As shown in Figure 2, for U_{60}/NaCl solutions, the scattered intensities remain relatively low for both Groups 2 and 3. For U_{60} with RbCl or CsCl, the blackberry sizes are almost the same as they were in Group 1, whereas for U_{60}/KCl, the assembly sizes of Group 2 are similar to Group 1. However, the blackberry size of the Group 3 solutions shows a noticeable increase compared to Group 1. Overall, only the pre-incubated U_{60} solutions with K^+ ions can respond to the temperature change before blackberry formation. These results clearly demonstrate the role of hydration layers during the self-assembly of U_{60}. The thinner

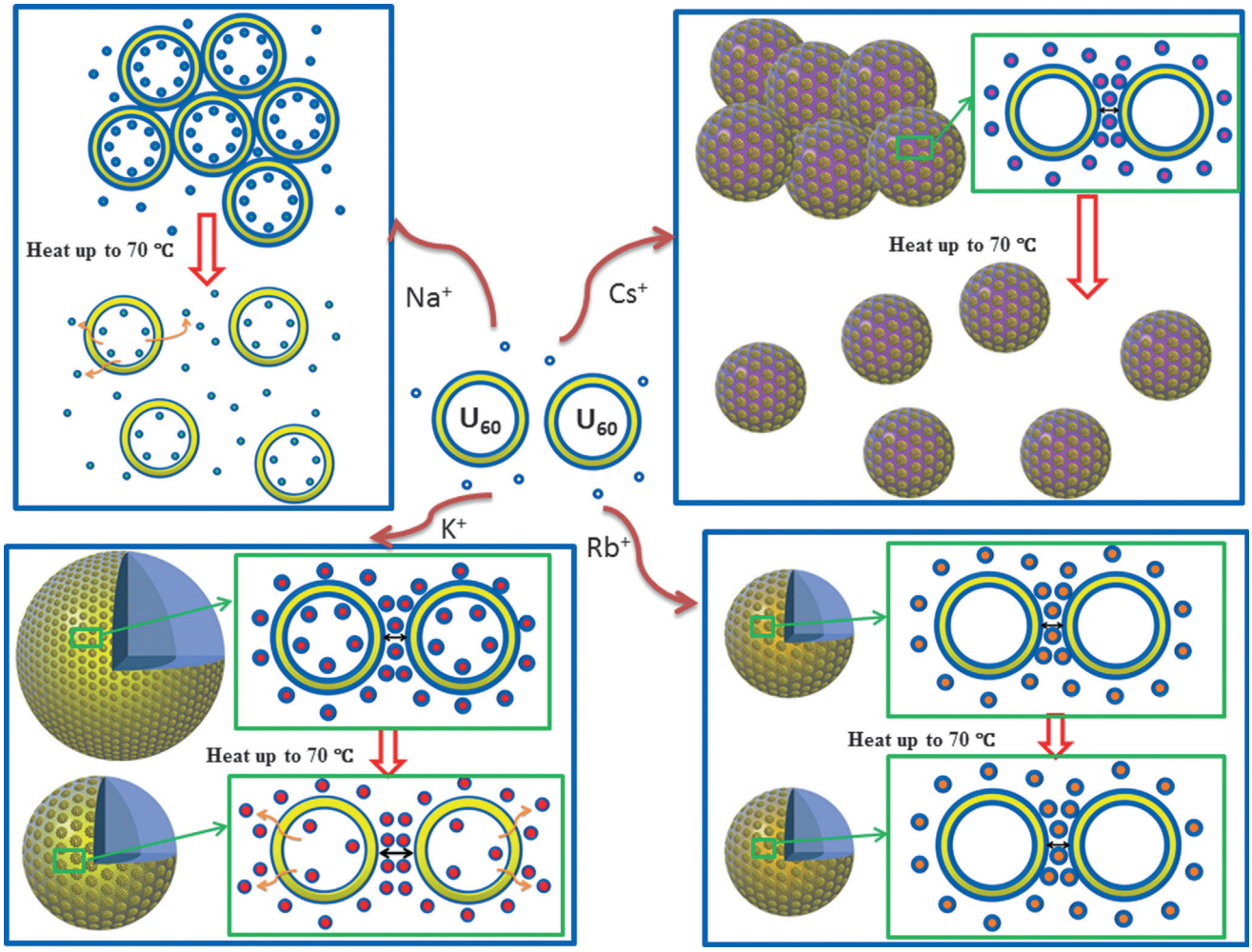

Figure 3. U_{60} clusters respond to additional alkali ions. For NaCl, U_{60} clusters tend to aggregate and precipitate at room temperature. When the temperature reaches 70 °C, U_{60} clusters are dispersed and become soluble again. For KCl, blackberries form in solution. Raising the temperature leads to a smaller blackberry size. For RbCl, blackberries form at room temperature and remain the same at 70 °C. For CsCl, U_{60} firstly self-assembles into blackberries, which gradually aggregate and precipitate. After heating the solution up to 70 °C, aggregated blackberries are separated from each other in solution. Key: U_{60} clusters (yellow circles); hydration shells (blue corona); Li^+, K^+, Rb^+, and Cs^+ counterions (cyan, red, orange, and purple dots, respectively).

hydration layer at 50 °C makes U_{60} more permeable to transport of K^+ ions, and thus more K^+ ions are able to enter the U_{60} cages after pre-incubation. This phenomenon leads to a lower surface charge of U_{60}, and finally, a larger blackberry size (Figure 4).

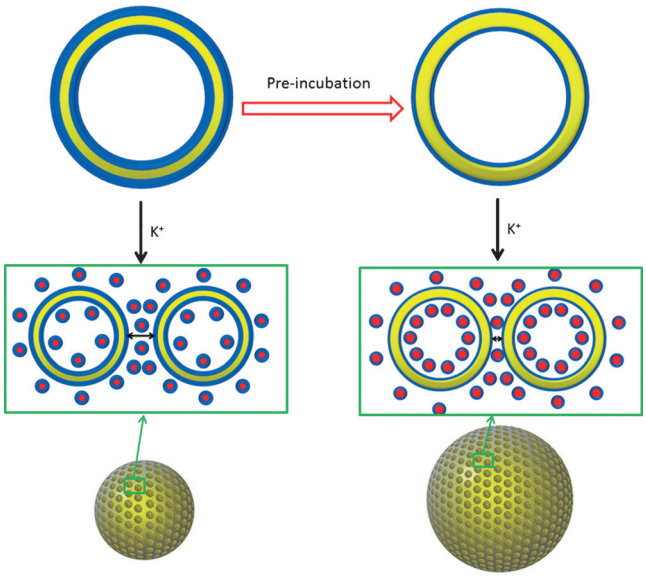

Figure 4. After pre-incubation, the hydration shell (blue corona) of U_{60} clusters (yellow circle) is reduced so that more K^+ ions are able to enter the inner cage of U_{60}. The diffusion of K^+ ions is extremely fast and goes to completion before blackberry are formed.

Moreover, the diffusion of K^+ ions into U_{60} cages is extremely fast, which is another important feature shared with K^+ ion channels.[1] Compared with Group 3, Group 2 was immediately placed at 50 °C after titration. However the blackberry sizes all remained the same, as in the reference group. This observation indicates that the K^+ diffusion process must be exceedingly fast so that it can conclude before the hydration layers are impacted by the high temperature. Therefore, the assembly size is only determined by the initial hydration state of U_{60} clusters when interacting with counterions. The diffusion of K^+ ions into the U_{60} cages finishes immediately after they are added to the solution, and before blackberry formation.

Groups 2 and 3 were then heated at 70 °C. For both KCl groups, the size of blackberries showed a clear drop at 70 °C, while the NaCl, RbCl, and CsCl groups demonstrated no noticeable change in blackberry size (Figure 2). This confirms our earlier speculation that some of the trapped K^+ ions can migrate into the bulk solution from the U_{60} cage when the temperature rises, but are not capable of moving back.

The ion selectivity model is further supported by an ITC study. NaCl, KCl, RbCl, and CsCl solutions were titrated into U_{60} (1.0 mg mL^{-1}) solutions. One set of solutions was titrated at 50 °C directly after preparation at room temperature, as in Group 2. The other set was pre-incubated at 50 °C for 3 days before running ITC, as in Group 3. The results, shown in Table 1 and Table 2, explicitly suggest the following; 1) unlike

Table 1: ITC results of non-pre-incubated U_{60} solutions at 50 °C (Group 2).

	NaCl	KCl	RbCl	CsCl
ΔH [kJ mol^{-1}]	−9.6	−16.4	−17.1	−21.2
ΔS [J mol^{-1} K^{-1}]	34.0	12.2	9.5	−0.8
ΔG [kJ mol^{-1}]	−20.6	−20.3	−20.1	−20.9

Table 2: ITC results of pre-incubated U_{60} solutions at 50 °C (Group 3).

	NaCl	KCl	RbCl	CsCl
ΔH [kJ mol^{-1}]	/	−7.3	−7.2	−10.7
ΔS [J mol^{-1} K^{-1}]	/	44.9	47.0	29.2
ΔG [kJ mol^{-1}]	/	−21.8	−22.3	−20.1

KCl, the heat level of U_{60} with NaCl in Group 3 is as low as the background level and cannot be properly fitted, indicating that there are no noticeable interactions between U_{60} and Na^+ ions when the temperature reaches 50 °C. This is consistent with our previous observations and proves that U_{60} can distinguish between Na^+ and K^+ at 50 °C. 2) The entropy change (ΔS) becomes much more positive after pre-incubation. The entropy change of the U_{60} binding process mainly arises from the destruction of U_{60} hydration shells.[9] This result indicates that, although the thickness of hydration shells are compromised by pre-incubation, the excess K^+ ions coming out of the U_{60} cages compensate for the entropy loss and thereby create a higher entropy level for the whole system.

Subsequently, we considered what would happen if the pre-incubation temperature were raised to further dehydrate the U_{60} clusters. Another set of solutions was studied using a pre-incubation temperature of 70 °C (Group 4). Group 4 shows a noteworthy phenomenon: while the CsCl assembly size remained the same, the size of RbCl and KCl assemblies increased incrementally (Figure 2; Supporting Information, Table S4). The size increase caused by Rb^+ reveals that Rb^+ ions can also enter the cages of U_{60} after a 70 °C pre-incubation because of a thinner hydration shell and lower effective charge of U_{60}.

In summary, U_{60} clusters demonstrate tunable ion selectivity at different temperatures that can mimic the function of protein ion channels. At room temperature, U_{60} clusters allow Na^+ and K^+ ions to pass through the surface pores. When the temperature is around 50 °C, only K^+ ions are able to enter the inner space, whereas after pre-incubation at 70 °C, both K^+ and Rb^+ diffused into the U_{60} cage. The tailorable permeability for different alkali ions is mainly attributed to the thermal responsiveness of the U_{60} cluster's hydration shells. At high temperatures, some trapped K^+ ions can be released from the U_{60} cages as a result of higher kinetic energy and a thinner hydration shell. However, once ions are released, it is difficult for them to return to the cages. K^+ ions can only enter the U_{60} cages when they exist as discrete ions (or oligomers). Once U_{60} clusters are self-assembled, they no longer allow K^+ ions to diffuse into the cage. Generally, U_{60} clusters share various properties with classical K^+ channels: (1) the transport of K^+ ions is passive;[15] (2) the diffusion rate

of K^+ ions is extremely fast; (3) to successfully pass through the surface pore, dehydration of both U_{60} and K^+ is necessary;[16] (4) most importantly, the U_{60} clusters are able to distinguish between Na^+ and K^+ ions with high precision at specific temperatures.

Acknowledgements

This material is based upon work supported by the Materials Science of Actinides Center, an Energy Frontier Research Center funded by the U.S. Department of Energy, Office of Science, Office of Basic Energy Sciences under Award Number DE-SC0001089.

Keywords: ion channels · ion selectivity · self-assembly · uranyl peroxide nanocages

How to cite: *Angew. Chem. Int. Ed.* **2016**, *55*, 6887 – 6891
Angew. Chem. **2016**, *128*, 7001 – 7005

[1] E. Gouaux, R. MacKinnon, *Science* **2005**, *310*, 1461 – 1465.
[2] a) D. A. Doyle, J. M. Cabral, R. A. Pfuetzner, A. Kuo, J. M. Gulbis, S. L. Cohen, B. T. Chait, R. MacKinnon, *Science* **1998**, *280*, 69 – 77; b) F. I. Valiyaveetil, M. Leonetti, T. W. Muir, R. MacKinnon, *Science* **2006**, *314*, 1004 – 1007; c) S. Y. Noskov, S. Berneche, B. Roux, *Nature* **2004**, *431*, 830 – 834.
[3] a) R. Carr, I. A. Weinstock, A. Sivaprasadarao, A. Müller, A. Aksimentiev, *Nano Lett.* **2008**, *8*, 3916 – 3921; b) A. Gilles, M. Barboiu, *J. Am. Chem. Soc.* **2015**, *138*, 426-432; c) Z. Sun, M. Barboiu, Y. M. Legrand, E. Petit, A. Rotaru, *Angew. Chem. Int. Ed.* **2015**, *54*, 14473 – 14477; *Angew. Chem.* **2015**, *127*, 14681 – 14685; d) M. Nyman, T. M. Alam, *J. Am. Chem. Soc.* **2012**, *134*, 20131 – 20138.
[4] a) P. Yang, Y. Xiang, Z. Lin, B. S. Bassil, J. Cao, L. Fan, Y. Fan, M. X. Li, P. Jiménez-Lozano, J. J. Carbó, *Angew. Chem. Int. Ed.* **2014**, *53*, 11974 – 11978; *Angew. Chem.* **2014**, *126*, 12168 – 12172; b) C. Streb, D.-L. Long, L. Cronin, *Chem. Commun.* **2007**, 471 – 473; c) A. Merca, H. Bögge, M. Schmidtmann, Y. Zhou, E. T. Haupt, M. K. Sarker, C. L. Hill, A. Müller, *Chem. Commun.* **2008**, 948 – 950; d) A. Ziv, A. Grego, S. Kopilevich, L. Zeiri, P. Miro, C. Bo, A. Müller, I. A. Weinstock, *J. Am. Chem. Soc.* **2009**, *131*, 6380 – 6382.
[5] E. Mahon, S. Garai, A. Müller, M. Barboiu, *Adv. Mater.* **2015**, *27*, 5165 – 5170.
[6] O. Petina, D. Rehder, E. T. Haupt, A. Grego, I. A. Weinstock, A. Merca, H. Bögge, J. Szakács, A. Müller, *Angew. Chem. Int. Ed.* **2011**, *50*, 410 – 414; *Angew. Chem.* **2011**, *123*, 430 – 434.
[7] a) P. Miro, C. Bo, *Inorg. Chem.* **2012**, *51*, 3840 – 3845; b) E. Tiferet, A. Gil, C. Bo, T. Y. Shvareva, M. Nyman, A. Navrotsky, *Chem. Eur. J.* **2014**, *20*, 3646 – 3651.
[8] G. E. Sigmon, D. K. Unruh, J. Ling, B. Weaver, M. Ward, L. Pressprich, A. Simonetti, P. C. Burns, *Angew. Chem. Int. Ed.* **2009**, *48*, 2737 – 2740; *Angew. Chem.* **2009**, *121*, 2775 – 2778.
[9] Y. Gao, F. Haso, J. E. Szymanowski, J. Zhou, L. Hu, P. C. Burns, T. Liu, *Chem. Eur. J.* **2015**, *21*, 18785 – 18790.
[10] a) J. Israelachvili, H. Wennerström, *Nature* **1996**, *379*, 219 – 225; b) S. Ebbinghaus, S. J. Kim, M. Heyden, X. Yu, U. Heugen, M. Gruebele, D. M. Leitner, M. Havenith, *Proc. Natl. Acad. Sci. USA* **2007**, *104*, 20749 – 20752; c) P. Miró, B. Vlaisavljevich, A. L. Dzubak, S. Hu, P. C. Burns, C. J. Cramer, R. Spezia, L. Gagliardi, *J. Phys. Chem. C* **2014**, *118*, 24730 – 24740.
[11] J. A. Soltis, C. M. Wallace, R. L. Penn, P. C. Burns, *J. Am. Chem. Soc.* **2015**, *138*, 191-198.
[12] a) P. Yin, D. Li, T. Liu, *Chem. Soc. Rev.* **2012**, *41*, 7368 – 7383; b) G. Liu, T. Liu, *Langmuir* **2005**, *21*, 2713 – 2720; c) T. Liu, B. Imber, E. Diemann, G. Liu, K. Cokleski, H. Li, Z. Chen, A. Müller, *J. Am. Chem. Soc.* **2006**, *128*, 15914 – 15920; d) M. L. Kistler, A. Bhatt, G. Liu, D. Casa, T. Liu, *J. Am. Chem. Soc.* **2007**, *129*, 6453 – 6460; e) J. M. Pigga, J. A. Teprovich, R. A. Flowers, M. R. Antonio, T. Liu, *Langmuir* **2010**, *26*, 9449 – 9456.
[13] G. Liu, Y. Cai, T. Liu, *J. Am. Chem. Soc.* **2004**, *126*, 16690 – 16691.
[14] a) A. A. Zavitsas, *J. Phys. Chem. B* **2005**, *109*, 20636 – 20640; b) X. Xu, G. Shan, Y. Shang, P. Pan, *J. Appl. Polym. Sci.* **2014**, *131*, 40589.
[15] R. MacKinnon, *Angew. Chem. Int. Ed.* **2004**, *43*, 4265 – 4277; *Angew. Chem.* **2004**, *116*, 4363 – 4376.
[16] Y. Zhou, J. H. Morais-Cabral, A. Kaufman, R. MacKinnon, *Nature* **2001**, *414*, 43 – 48.

Received: February 22, 2016
Revised: March 26, 2016
Published online: April 23, 2016

